An Investigation of the Ligand-Binding Site of the Glutamine-Binding Protein of *Escherichia coli* Using Rotational-Echo Double-Resonance NMR†

Andrew W. Hing,‡ Nico Tjandra,§ Patricia F. Cottam,§ Jacob Schaefer,*,‡ and Chien Ho*,§

Department of Chemistry, Washington University, 1 Brookings Drive, St. Louis, Missouri 63130, and Department of Biological Sciences, Carnegie Mellon University, 4400 Fifth Avenue, Pittsburgh, Pennsylvania 15213

Received February 14, 1994®

ABSTRACT: Glutamine-binding protein (GlnBP) is an essential component of the glutamine transport system in *Escherichia coli*. Rotational-echo double-resonance (REDOR) solid-state nuclear magnetic resonance (NMR) has been used to determine internuclear distances in the complex of GlnBP and its ligand, L-glutamine. REDOR, combined with strategically placed isotopic labels, is effective in obtaining model-independent internuclear distances and thus detailed structural information on the ligand-binding site of GlnBP. The existence of a single histidine residue (His156) in the binding site has provided an excellent probe for distance measurements between protein and ligand. REDOR distances up to 6.3 Å have been observed between ^{13}C labels in L-glutamine and ^{15}N labels in His156. These results have unambiguously determined the ligand orientation with respect to the imidazole ring of His156, which is an important first step in refining the ligand-binding-site model of GlnBP in general. The measured distances were also used as constraints in restrained molecular dynamics calculations of the complex using the unliganded crystal structure of GlnBP as the starting point. The simulations clearly show consistency between calculated distances and those measured by REDOR.

Periplasmic binding proteins are integral parts of complex osmotic shock-sensitive membrane transport systems in Gram-negative bacteria (Neu & Heppel, 1965). These membrane transport systems belong to a superfamily of transport systems known as traffic ATPases (Ames *et al.*, 1990), also known as ATP[1]-binding cassette transporters (Hyde *et al.*, 1990). A model of these transport systems has been proposed by Ames (1986). This model is composed of a ligand-specific periplasmic protein and two or three membrane-bound protein components. Each periplasmic protein has a very high affinity and specificity for its ligand. These properties are presumably governed by hydrogen-bond acceptors and the geometry of the ligand-binding site (Vyas *et al.*, 1983; Luecke & Quiocho, 1990). These factors ensure the efficiency of the overall transport process.

All periplasmic binding proteins whose crystal structures have been determined have been found to have a similar two-domain, hinged structure in which the cleft between the two domains provides the ligand-binding site (Quiocho, 1990). Upon ligand binding, these two domains undergo a conformational change which is primarily due to the hinge-bending motion (Newcomer *et al.*, 1981; Mao *et al.*, 1982). This motion closes the cleft and a very compact globular structure is formed. This conformational change is believed to be an important factor in the recognition of the periplasmic binding protein–ligand complex by membrane-bound protein components. This recognition is an initial step in the translocation of the ligand across the membrane (Ames, 1986; Quiocho, 1990). Even though the general features of this type of active transport process are known, the detailed molecular mechanisms and the important aspects for ligand recognition or protein–protein interactions are still not very well understood. An important question which needs to be addressed is the origin of the specificity that each periplasmic binding protein shows for its ligand, even though the three-dimensional crystal structures of all these binding proteins indicate common structural features (Quiocho, 1990).

In this study, we examine the glutamine-binding protein (GlnBP) of *Escherichia coli*. GlnBP binds L-glutamine with a dissociation constant of 5×10^{-7} M at 5 °C and pH 7.2 (Shen *et al.*, 1989a). GlnBP is a monomeric protein with 226 amino acid residues and a molecular weight of 24 935. It is an integral part of the glutamine transport system in Gram-negative bacteria, which is one of the most studied bacterial transport systems (Weiner & Heppel, 1971; Kreishman *et al.*, 1973; Hunt & Hong, 1981, 1983a; Nohno *et al.*, 1986; Shen *et al.*, 1989a,b). The transport system is specific for L-glutamine (Weiner & Heppel, 1971; Willis *et al.*, 1975). GlnBP is stable with respect to changes in pH and temperature (Shen *et al.*, 1989a,b). A crystallographic investigation of unliganded GlnBP has been carried out (Chen *et al.*, 1989; Hsiao, 1993; Hsiao *et al.*, 1994). However, crystal data on the complex of GlnBP and L-Gln are not yet available. High-resolution ^1H-NMR spectra show the formation of an intermolecular hydrogen bond between L-Gln and GlnBP (Shen *et al.*, 1989a). Further analysis of this hydrogen bond has suggested that the location of the ligand-binding site of GlnBP involves $N_{\epsilon 2}$-H of His156 (Shen *et al.*, 1989a; Tjandra

† Supported by research grants from the National Science Foundation (DMB-8816384 to C.H.) and the National Institutes of Health (GM-26874 to C.H., GM-40634 to J.S.), and Grant RR-02231 to the National Stable Isotopes Resources at the Los Alamos National Laboratory, which provided the L-[*ring*-2-^{13}C]histidine used in this study. This material was presented in part at the 38th Annual Meeting of the Biophysical Society held on March 6–10, 1994, in New Orleans, LA.

* To whom correspondence should be addressed.

‡ Washington University.

§ Carnegie Mellon University.

® Abstract published in *Advance ACS Abstracts,* July 1, 1994.

[1] Abbreviations: GlnBP, glutamine-binding protein; REDOR, rotational-echo double resonance; NMR, nuclear magnetic resonance; ATP, adenosine 5′-triphosphate; SEDOR, spin-echo double resonance; MOPS, 3-(*N*-morpholino)propanesulfonic acid; DSS, 2,2-dimethyl-2-silapentane-5-sulfonate; TMS, tetramethylsilane; CPMAS, cross-polarization magic-angle spinning; CP, cross polarization; MAS, magic-angle spinning; MeA, α-methylalanine; *D*, dipolar coupling; *L*, percent of isotopically labeled ligand; N_c, number of rotor cycles; *S*, dephased spectrum; S_0, full-echo spectrum; ΔS, difference spectrum; T_r, rotor period; *M*, correction factor for REDOR performance.

0006-2960/94/0433-8651$04.50/0

et al., 1992). The working model for this analysis assumed that one of the intermolecular hydrogen bonds that forms in the GlnBP–L-Gln complex is between the $H_{\epsilon 2}$ of His156 and the γ-carboxyl group of the L-glutamine ligand.

In solution NMR, the determination of dipolar couplings between protons separated by less than 5 Å provides distances to characterize the geometry of structures of proteins (Wüthrich, 1989). As the size of the protein increases, the selectivity of this type of measurement decreases rapidly. This is due to (i) spectral overlap, (ii) the complexity of the strong dipolar coupling networks among many protons, and (iii) the dependence of the derived distance on the dynamic model chosen for the system. Recent advances in the design of pulse sequences, improvements in spectrometers, strategies involving three- and/or four-dimensional NMR, and ^{15}N and/or ^{13}C enrichment of the protein under study have all been used in an attempt to overcome the first problem [for recent reviews, see Clore and Gronenborn (1991) and Bax and Grzesiek (1993)]. Current methods of data analysis such as iterative back-calculation have minimized the second problem and perhaps a big part of the third problem (Boelens *et al.*, 1988, 1989; Koning, 1990). However, the present solution-state NMR approach is still limited to proteins of about 30 000 Da.

Dipolar coupling measurements on an immobilized protein reduce the dependence of the interpretation of the data on the dynamic model of the system. The use of selective isotopic labeling, i.e., isolated pairs of nuclei in a solid sample, provides a sensitive probe for internuclear distance measurement, in addition to reducing the complexity of the observed spectra. The distance measurement is carried out using spin-echo double resonance (SEDOR) (Shore *et al.*, 1987) and its magic-angle spinning variation, rotational-echo double resonance (REDOR) (Gullion & Schaefer, 1989; Pan *et al.*, 1990). The latter method has been used in determining an enzyme–inhibitor interaction within the binding site (Christensen & Schaefer, 1993; Schmidt *et al.*, 1993) as well as the internuclear distances in a binding protein (McDowell *et al.*, 1993). In this study, the REDOR-NMR method has been used to determine internuclear distances in a lyophilized form of the complex between GlnBP and L-Gln.

MATERIALS AND METHODS

Emerimicin Preparation

Ac-Phe-[1-^{13}C]MeA-MeA-MeA-Val-[^{15}N]Gly-Leu-MeA-MeA-O-Bzl (emirimicin 1–9, the benzyl ester) of the amino-terminal portion of the peptide antibiotics emirimicins III and IV was prepared using the method described by Marshall *et al.* (1990).

Preparation of Glutamine-Binding Protein

Samples studied were composed of uniform or specifically isotopically labeled GlnBP bound to specific isotopically labeled L-Gln. GlnBP that was uniformly ^{15}N-enriched was prepared by a procedure described by Tjandra *et al.* (1992). For uniformly ^{15}N-depleted and L-[*ring*-2-^{13}C]His-labeled GlnBP, 20 mg/L L-[*ring*-2-^{13}C]His (kindly provided by Los Alamos National Laboratory) was added to the minimal medium and 0.7 g/L ^{15}N-depleted $^{14}NH_4{}^{14}NO_3$ was used as the nitrogen source to grow a histidine auxotroph (TA4260, a gift from Dr. G. F. Ames, University of California at Berkeley, Berkeley, CA) which was transformed with plasmids pGT1–2 and pJW133 (a gift from Dr. J.-S. Hong, Boston Biomedical Research Institute, Boston, MA). For the preparation of ^{15}N-enriched, [*m*-^{19}F]Tyr-labeled GlnBP, a tyrosine auxotroph (AT2471 provided by Dr. Barbara Bachmann, *E. coli* Genetic Stock Center, New Haven, CT) was transformed with the same plasmids. The transformed cells were grown at 30 °C in 1 L of L-broth until early to mid log phase. The culture was centrifuged, and the pellet was resuspended in 10 mL of supernatant, inoculated into 5 L of minimal glucose medium containing 0.7 g/L $(^{15}NH_4)_2SO_4$ as a nitrogen source, and supplemented with 4 mg/L L-Tyr. Following a 5-h incubation with rapid aeration, 40 mg/L DL-[*m*-^{19}F]Tyr (Sigma, St. Louis, MO) was added and growth continued for an additional 16 h prior to heat induction of the T7 polymerase. L-Gln used in this study included L-[5-^{13}C]-Gln (MSD Isotopes, St. Louis, MO), L-[amide-^{15}N]Gln (MSD Isotopes, St Louis, MO), L-[*amine*-^{15}N]Gln (CIL, Woburn, MA), and L-Gln at natural abundance (Aldrich, Milwaukee, WI). All labels were 98% or greater enrichment.

GlnBP and L-Gln were complexed by mixing a 1:3 molar ratio of isotopically labeled GlnBP and the appropriate labeled L-Gln in the presence of 2 mM 3-(*N*-morpholino)propanesulfonic acid (MOPS) (Sigma, St. Louis, MO) at pH 7.2. The mixture was then washed with at least 100 times the sample volume of the same MOPS buffer to get rid of the excess ligand in the sample. This procedure resulted in the binding of protein to ligand in a 1:1 ratio. This was verified by high-resolution ^1H-NMR examination of the location of the N_1-H resonance of Trp220 in the protein, which showed no residual resonance line at 11.12 ppm from 2,2-dimethyl-2-silapentane-5-sulfonate (DSS) (Sigma, St. Louis, MO), corresponding to the unliganded GlnBP (Shen *et al.*, 1989a), and by high-resolution ^{13}C-NMR examination of the location of the $^{13}C_\delta$ resonance of the L-Gln ligand, which showed no residual resonance line at 177.5 ppm from tetramethylsilane (TMS) (Sigma, St. Louis, MO), corresponding to the unbound ligand (results not shown).

Samples for cross-polarization magic-angle spinning (CP-MAS) echo experiments were lyophilized from a solution whose MOPS concentration at pH 7.2 was varied while the protein–ligand complex was maintained at a 1 mg/mL concentration. Samples for REDOR experiments were lyophilized using a shell–freeze procedure from 2 mM MOPS buffer at pH 7.2 in which the protein–ligand complex was dissolved at a 1 mg/mL concentration. A lyophilization period of at least 48 h ensures a minimal water content in the sample.

As a control, an unlabeled and unliganded wild-type GlnBP sample was checked by 500-MHz ^1H-NMR spectroscopy for the ability to bind ligand, and for any resonance broadening, at different stages of solid-state sample preparation and after the completion of a REDOR experiment. This was done in order to make sure that the protein was still in the native and active conformation after such treatment.

NMR

NMR Console and Probe. Solid-state NMR experiments involving nonfluorinated samples were performed with a three-channel spectrometer and probe operating at 200 MHz (^1H), 50 MHz (^{13}C), and 20 MHz (^{15}N). This spectrometer has been previously described (Marshall *et al.*, 1990). NMR experiments involving the fluorinated sample were performed with a four-channel spectrometer and probe operating at 200 MHz (^1H), 188 MHz (^{19}F), 50 MHz (^{13}C), and 20 MHz (^{15}N), which also has been previously described (Holl et al., 1992). High-resolution, solution-state spectra were obtained with a Bruker AM-500 spectrometer using a broad-band probe tuned specifically for ^1H, ^{13}C, or ^{15}N.

General Acquisition Parameters. NMR spectra were acquired at a MAS speed of $1/T_r$ = 3759 Hz. Cross

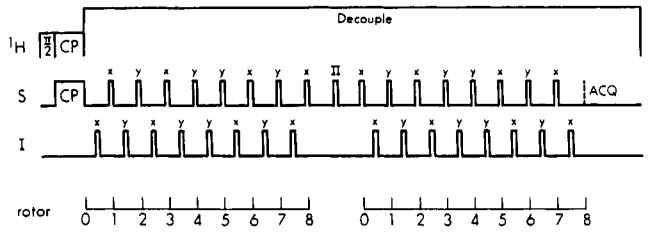

FIGURE 1: REDOR pulse sequence using the XY-8 phase-cycling scheme for both rare-spin channels. The S-spin signal is acquired with refocusing of isotropic chemical shifts, and N_c, the number of rotor cycles with dephasing, is a multiple of 8.

polarization (CP) was performed at a field strength of 38 kHz with a contact time of 2 ms. The 90° pulse width was 6.6 μs for ^{1}H, ^{19}F, ^{13}C, and ^{15}N. Spectra were referenced to an external standard and were acquired with a spectral width of 20 000 Hz, a spectral size of 2048 complex points, a recycle delay of 1 s, and a ^{1}H decoupling field strength of approximately 100 kHz. Spectra were processed with a line broadening of 40 Hz and plotted with a spectral width of 10 000 Hz. Data were acquired at room temperature (25 °C).

^{15}N-CPMAS Echo. ^{15}N-CPMAS echo spectra were acquired with phase cycling of the ^{15}N-CP pulse, the rotor-synchronized refocusing 180° pulse, and the receiver reference frequency following the scheme of Rance and Byrd (1983). The proton spin temperature was alternated between consecutive scans.

^{13}C,^{15}N-REDOR. The REDOR pulse sequence used in this paper is diagramed in Figure 1. The initial cross polarization from protons to S-spins is followed by a train of S-spin π pulses, each of which is applied at the end of a rotor period, a train of I-spin π pulses, each of which is applied at a time $T_r/2$ from the start or end of a rotor period, and high-power proton decoupling. During data acquisition, the I-spin π pulses are alternately applied or removed from the sequence to create a dephased spectrum (S) and a full-echo spectrum (S_0), respectively, that are recorded in separate memory blocks. The full-echo spectrum minus the dephased spectrum yields the difference spectrum (ΔS). The application of a train of π pulses to both S-spin and I-spin nuclei and phase alternation of each π-pulse train according to an XY-8, compensated Carr–Purcell scheme (Gullion *et al.*, 1990) are modifications of the original REDOR sequence (Gullion & Schaefer, 1989; Gullion *et al.*, 1990). The addition of an S-spin π pulse (denoted by Π in the sequence of Figure 1) to the XY-8 train of S-spin π pulses is required for full implementation of the XY-8 phase alternation scheme. Consequently, the total number of rotor periods of dephasing, N, is two less than the total number of rotor periods between the S-spin CP pulse and data acquisition. The phases of the XY-8 π pulses were left unchanged while phase cycling of the S-spin CP pulse, the π pulse, and the receiver reference frequency followed the scheme of Rance and Byrd (1983). The spin temperature was alternated between consecutive scans.

The REDOR pulse sequence in Figure 1 was modified slightly to acquire data on the fluorinated sample. Only the loop before the Π pulse was used for dephasing, and data acquisition was started exactly one rotor period after the Π pulse.

Molecular Refinement. The L-Gln ligand was interactively docked into the binding cavity of GlnBP using the SYBYL molecular modeling program (Tripos, St. Louis, MO) to an approximately correct distance to the His156 residue. The

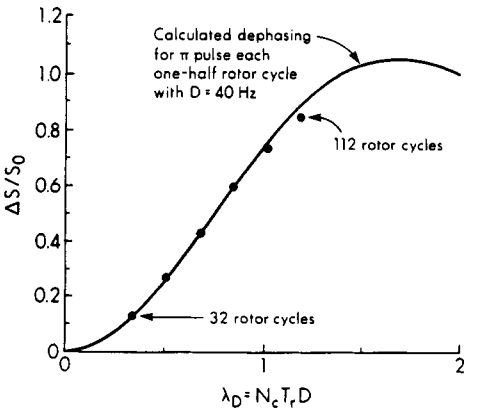

FIGURE 2: Observed dependence of carbonyl carbon $\Delta S/S_0$ on λ_D for a ^{13}C–^{15}N double-labeled emirimicin 1–9 benzyl ester. The parameter λ_D is the product of the number of rotor cycles with dephasing (N_c), the rotor period (T_r), and the ^{13}C–^{15}N dipolar coupling (D). The sample weighed approximately 60 mg, and 16 000 scans were used to acquire each S and S_0 spectrum. The REDOR difference, ΔS, is $S_0 - S$.

starting structure is the 2.5-Å-resolution crystal structure of the unliganded GlnBP protein provided by Hsiao (1993) and Hsiao *et al.* (1994). The structure of the complex was obtained using the REDOR internuclear distances as the constraints and molecular dynamics calculation using the CHARMM22 program. The calculation was carried out on an SGI Indigo (Silicon Graphics Inc., Mountain View, CA). A time step of 1 fs was employed. The SHAKE algorithm (van Gunsteren & Berendsen, 1977) was used to fix hydrogen-bond lengths throughout the simulation. The Verlet scheme (Verlet, 1967) was used for the calculation of velocities at each step. REDOR-measured distances were used as NOE constraints in simulation. A total of 12 000 time steps were used in a heating period after the minimization stage to equilibrate the temperature slowly to 300 K. Another 8000 time steps were used to equilibrate the overall system at 300 K. The equilibration was done prior to the 20 ps of total dynamics calculation. No water molecules were included in the calculation, since no crystal data on waters in the system are available at this time. A distance-dependent dielectric was used to compensate for the missing solvent. Structures were saved every 0.4-ps interval. The root-mean-square deviations of atoms from their mean positions were calculated from the trajectory analysis on the 50-saved structures.

RESULTS

Emerimicin

^{13}C-Observed, ^{15}N-Dephased REDOR. REDOR experiments were performed on Ac-Phe-[1-^{13}C]MeA-MeA-MeA-Val-[^{15}N]Gly-Leu-MeA-MeA-O-Bzl emerimicin fragment with 32, 48, 64, 80, 96, and 112 rotor cycles of dephasing in order to compare its performance to the theoretical values (Figure 2). The ^{13}C signal arising from the label in the emirimicin fragment is not resolved from that of natural-abundance peptide carbonyl carbons, which make a constant 7.7% contribution to the full echo signal, S_0. This correction can either be measured in a separate experiment on a natural-abundance sample or be calculated from the known structure. In addition, the natural-abundance ^{13}C carbonyls of Val5 and Gly6 are respectively one and two bonds away from the ^{15}N label and so will make a contribution to ΔS that reaches a maximum value of 2% by about $N_c = 16$. The other natural-abundance carbonyl ^{13}C's are all farther away from the ^{15}N label than is the carbonyl label at MeA2. Thus, the observed

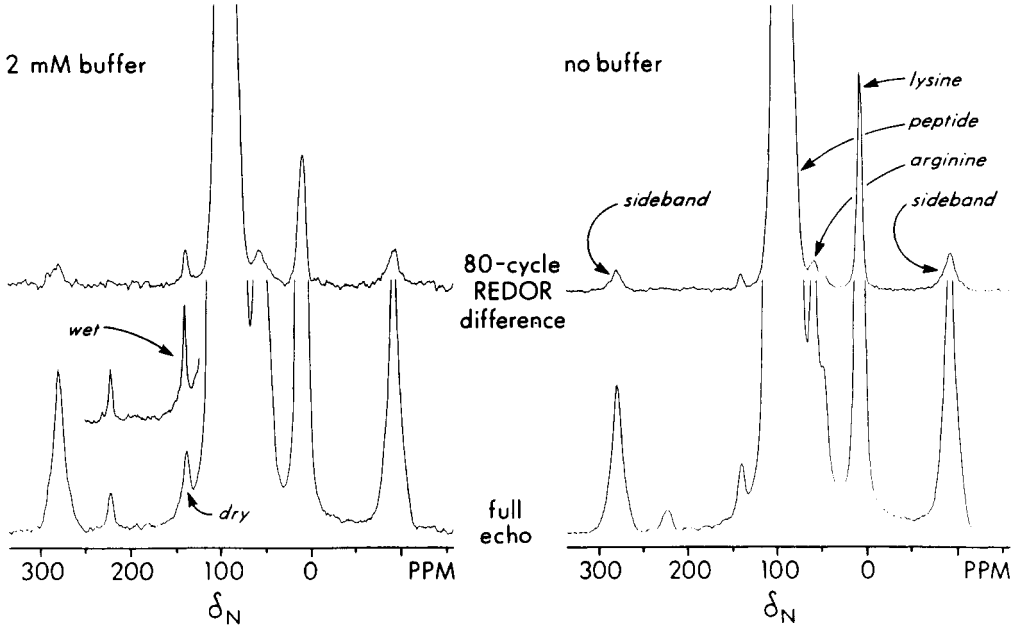

FIGURE 3: 20.3-MHz ^{15}N NMR full-echo spectrum (bottom) and REDOR difference (top) of [U-^{15}N]GlnBP bound to L-[5-^{13}C]Gln lyophilized from 0.05 mM protein–ligand complex solution in the presence of 2 mM MOPS buffer (left) and no buffer (right). Line widths of the two histidine [^{15}N]imidazole nitrogen peaks (140 and 220 ppm) depend on the presence of buffer. The full-echo insert shown on the left arose from an incompletely dried sample. The ϵ-amino peaks arise from the ζ nitrogens of lysines. The spectra were obtained using the pulse sequence of Figure 1 with $N_c = 80$.

Table 1: Summary of Line Widths of the Imidazole Nitrogens of His156 as a Function of Buffer Concentrations[a]

buffer concn (mM)	His156 $^{15}N_{\delta 1}$ line width (Hz)	His156 $^{15}N_{\epsilon 2}$ line width (Hz)
0.5	180	177
1	154	134
1.6	148	129
2	134	120
2.4	126	117

[a] Protein concentration prior to lyophilization was 1 mg/mL for every sample. Error of line-width measurements is less than 15%.

ΔS is dominated by the coupling of the ^{15}N–^{13}C labels, and additional natural-abundance corrections are unimportant for $N_c > 32$. The experimental results (solid circles) are in agreement with calculations (solid line) assuming a ^{13}C–^{15}N dipolar coupling of 40 Hz corresponding to a C–N distance of 4.2 ± 0.1 Å. The distance by X-ray analysis is 4.16 Å (Marshall *et al.*, 1990). By $N_c = 96$, $\Delta S/S_0$ is greater than 0.7 with less than a 2-Hz natural-abundance correction for dipolar coupling (D). The agreement between X-ray and REDOR determinations of the [1-^{13}C]MeA2–[^{15}N]Gly6 distance for this calibration sample for $N_c = 8$ (Marshall *et al.*, 1990) to $N_c = 112$ (Figure 2) confirms that, with the compensation of the XY-8 phase-cycling scheme, hundreds of dephasing pulses can be used with no significant accumulation of error for a REDOR difference.

Glutamine-Binding Protein

^{15}N-CPMAS Echo. The results of REDOR experiments performed on [U-^{15}N]GlnBP bound to L-[5-^{13}C]Gln (the C-5 carbon of glutamine is C_δ) and to L-Gln are shown in Figure 3 and Table 1 as a function of the buffer concentration. As the buffer concentration of the solution to be lyophilized is increased, the line widths of the $^{15}N_{\epsilon 2}$ of the His156 signal (~140 ppm) and the $^{15}N_{\delta 1}$ of the His156 signal (~220 ppm) decrease (Table 1). This indicates that the local conformational environment of the His156 site increases in homogeneity as the ratio of buffer to protein–ligand complex increases and that a minimum number of buffer counterions should be present during lyophilization to yield the most homogeneous molecular environment (Christensen & Schaefer, 1993). On the basis of these data, samples prepared for REDOR experiments were lyophilized from a 1 mg/mL protein solution whose buffer concentration was 2 mM. Figure 3 compares the spectrum of such a sample with that of a sample containing no buffer. An incompletely dried sample resulted in the particularly sharp full-echo $^{15}N_{\delta 1}$ as well as $^{15}N_{\epsilon 1}$ of the His156 signals (Figure 3, left, middle insert), but this degree of narrowing was not routinely oberved.

^{15}N-Observed, ^{13}C-Dephased REDOR of [U-^{15}N]GlnBP + L-[5-^{13}C]Gln. The results of a REDOR experiment performed on [U-^{15}N]GlnBP bound to L-[5-^{13}C]Gln with $N_c = 48$ rotor cycles of dephasing are shown in Figure 4 (left), which displays the full-echo spectrum (bottom) and the difference spectrum (top). The full-echo spectrum is dominated by the large peak in the center and the accompanying MAS side bands representing mostly backbone [^{15}N]amide nitrogens. The difference spectrum represents those nitrogens that interact with a ^{13}C neighbor via dipolar coupling. Along with [^{15}N]amide (95 ppm), His156 (140 ppm), and lysine ϵ-amino peaks (10 ppm), arginine peaks in the vicinity of ~50 ppm are also visible in the difference spectrum. Intensities of the spinning side bands of these peaks indicate that there are no large-amplitude motions present in the lyophilized sample.

The determination of what proportion of the peak areas of the difference spectrum in Figure 4 (left) is due to interaction with $^{13}C_\delta$ of the L-Gln ligand and what proportion of the difference spectrum peak areas is due to interaction with ^{13}C nuclei present at natural abundance requires that a separate REDOR experiment be performed on a control sample consisting of [U-^{15}N]GlnBP bound to natural-abundance L-Gln. The results of such an experiment are shown in Figure 4 (right). Experimental conditions are identical to those in Figure 4 (left). The full-echo spectrum in Figure 4 (right) is virtually identical to that in Figure 4 (left). However, the

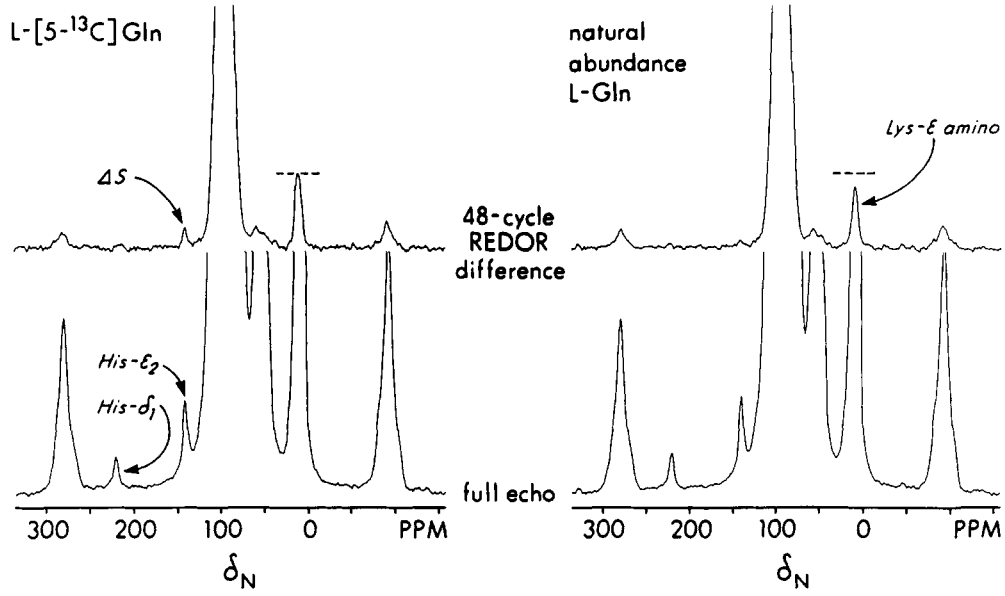

FIGURE 4: 20.3-MHz ^{15}N NMR full-echo spectrum (bottom) and REDOR difference (top) of 200 mg of [U-^{15}N]GlnBP bound to L-[5-^{13}C]Gln using 129 000 scans (left) and of 212 mg of [U-^{15}N]GlnBP bound to natural-abundance L-Gln using 214 000 scans (right). Both complexes were formed in the presence of 2 mM MOPS buffer. The spectra were obtained using the pulse sequence of Figure 1 with $N_c = 48$.

difference spectrum in Figure 4 (right) reveals the magnitude of ^{15}N dephasing by ^{13}C natural-abundance nuclei.

Determination of the distance between $^{15}N_{\epsilon 2}$ of His156 and $^{13}C_\delta$ of Gln by analysis of Figure 4 involves (i) division of the peak area at ~140 ppm in the difference spectrum by the peak area at ~140 ppm in the full-echo spectrum to obtain the values of $\Delta S/S_a = 0.28$ and $\Delta S/S_b = 0.11$ for Figure 4 (left) and Figure 4 (right), respectively; (ii) assumption of the suitability of direct subtraction of $\Delta S/S_b$ from $\Delta S/S_a$ to correct for background ^{13}C dephasing of the ^{15}N resonance; (iii) division by the percentage of isotopically labeled ligand present in the protein–ligand complex ($L = 0.804$) to correct for the presence of some natural-abundance ligand in the complex; (iv) conversion of $(\Delta S/S_a - \Delta S/S_b)/L = 0.21$ to the dimensionless quantity $N_c DT_r = 0.56$ (with D in hertz and T_r in seconds) according to standard REDOR tables; (v) calculation of $D = 37$ Hz; and (vi) calculation of the internuclear distance $r = 4.3$ Å according to the formula $r = (2894/D)^{1/3}$. This formula corresponds to an 875-Hz coupling for the 1.49-Å ^{13}C–^{15}N distance in L-[2-^{13}C,^{15}N]alanine. The percentage, $L = 0.804$, of isotopically labeled ligand present in the protein–ligand complex was determined by comparisons of ^{13}C-CPMAS-echo spin counts of the carbonyl carbons of the two samples of Figure 4. This was confirmed by ^{13}C high-resolution calibration of the $^{13}C_\delta$ enrichment of the complex using a known amount of L-[5-^{13}C]Gln as an external standard. This data analysis was done with the knowledge that the $N_{\delta 1}$ of His156 is not protonated, based on an earlier titration study of His156 (Tjandra, 1993).

Analysis of the data in Figure 4 to determine the distance between the ε-amino nitrogen (or N_ζ) of Lys and $^{13}C_\delta$ of Gln is predicated on the assumption that only one Lys residue is involved in the interaction with the $^{13}C_\delta$ of Gln. Data analysis proceeds as in the preceding paragraph, using the peak area at ~10 ppm. The result is multiplied by 28 to correct for the fact that the peak at ~10 ppm in the full-echo spectrum represents 28 different amines. Then $28(\Delta S/S_a - \Delta S/S_b)/L = 0.20$, $N_c DT_r = 0.45$, $D = 35$ Hz, and the internuclear distance $r = 4.4$ Å.

Further support for the above data analysis and its underlying assumptions is provided by repeating the experiments displayed by Figure 4, but with a different number of rotor cycles. The results of REDOR experiments performed on [U-^{15}N]GlnBP bound to L-[$^{13}C_\delta$]Gln or natural-abundance L-Gln with $N_c = 112$ rotor cycles of dephasing are shown in Figure 5. The results shown in Figures 4 and 5 are similar, except that the intensities of the difference signals are greater for larger N_c, as expected.

Analysis of Figure 5 to determine the distance between $^{15}N_{\epsilon 2}$ of His156 and $^{13}C_\delta$ of Gln shows that $\Delta S/S_a = 0.76$, $\Delta S/S_b = 0.13$, $(\Delta S/S_a - \Delta S/S_b)/L = 0.79$, $N_c DT_r = 1.07$, $D = 36$ Hz, and $r = 4.3$ Å. In fact, three determinations of the distance between $^{15}N_{\epsilon 2}$ of His156 and $^{13}C_\delta$ of Gln performed at $N_c = 48$, $N_c = 80$, and $N_c = 112$ rotor cycles yielded essentially the same internuclear distance: $r = 4.3 \pm 0.2$ Å (Table 2).

Analysis of the data in Figure 5 to determine the distance between $^{15}N_\zeta$ of Lys and $^{13}C_\delta$ of Gln shows that $28(\Delta S/S_a - \Delta S/S_b)/L = 0.80$ and that $N_c DT_r = 1.08$, $D = 36$ Hz, $r = 4.3$ Å. Three determinations of the distance between $^{15}N_\zeta$ of Lys and $^{13}C_\delta$ of Gln performed at $N_c = 48$, $N_c = 80$, and $N_c = 112$ rotor cycles gave the same internuclear distance $r = 4.4 \pm 0.2$ Å (Table 2), thereby justifying the assumption that only one lysine residue is involved in the interaction with the L-Gln ligand. In contrast, if there were more than one lysine residue involved, the amount of dephasing observed as a function of rotor cycles would deviate significantly from the calculated values given in Figure 2, and the distances determined by dephasing using different numbers of rotor cycles would not be in agreement.

Although the difference spectra of Figures 4 (left) and 5 (left) show a hint of a REDOR difference signal at ~220 ppm, the poor signal-to-noise ratio does not permit determination of the distance between $^{15}N_{\delta 1}$ of His156 and $^{13}C_\delta$ of L-Gln. The small $\Delta S/S$ suggests that the distance is more than 6.5 Å (Table 3).

^{15}N-Observed, ^{13}C-Dephased REDOR of L-[*ring*-2-^{13}C]-*His*-[*U*-^{14}N]*GlnBP* + L-[*Amide*-^{15}N]*Gln*. A REDOR experiment on L-[*ring*-2-^{13}C]His-[U-^{14}N]GlnBP bound to L-[*amide*-^{15}N]Gln with $N_c = 112$ rotor cycles was performed. The full-echo spectrum (results not shown) was dominated by a large peak in the center, which represents mostly [^{15}N]-amide of the glutamine ligand but may also contain a small component of the backbone [^{15}N]amide nitrogens even though

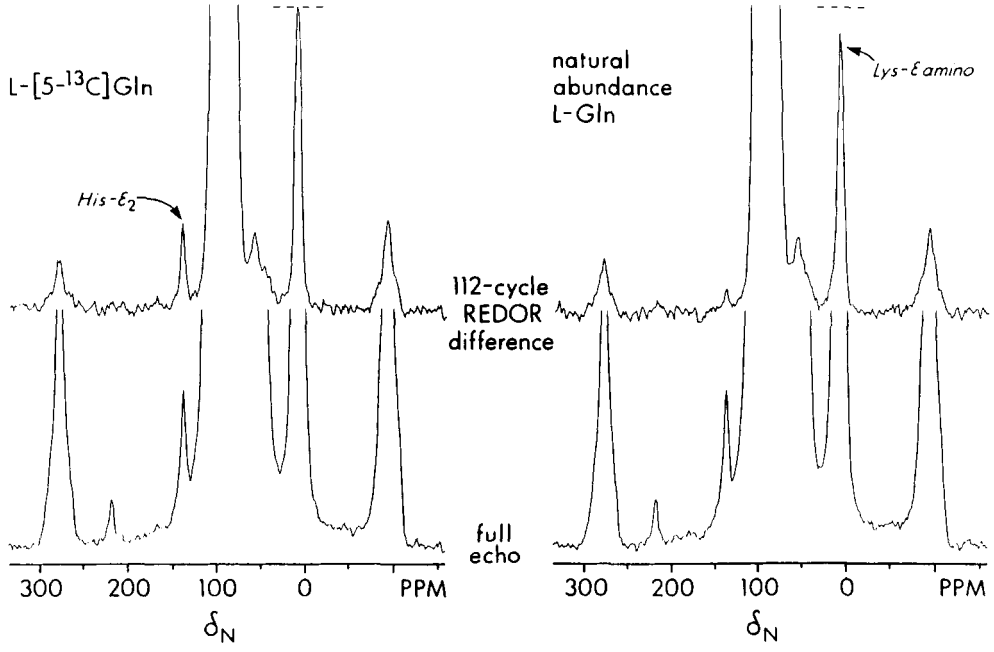

FIGURE 5: 20.3-MHz ^{15}N NMR full-echo spectrum (bottom) and REDOR difference (top) of 200 mg of [U-^{15}N]GlnBP bound to L-[5-^{13}C]Gln using 178 000 scans (left) and of 212 mg of [U-^{15}N]GlnBP bound to natural-abundance L-Gln using 162 000 scans (right). Both complexes were formed in the presence of 2 mM MOPS buffer. The spectra were obtained using the pulse sequence of Figure 1 with $N_c = 112$.

Table 2: Summary of REDOR Distances Measured with the [U-^{15}N]GlnBP + L-[5-^{13}C]Gln Sample

dephasing nucleus	obsd nucleus	rotor cycles of dephasing	$\Delta S/S_0$	REDOR distance (Å)
C_δ of L-Gln	$N_{\epsilon 2}$ of His156	48	0.21	4.3
C_δ of L-Gln	$N_{\epsilon 2}$ of His156	80	0.41	4.5
C_δ of L-Gln	$N_{\epsilon 2}$ of His156	112	0.79	4.3
C_δ of L-Gln	N_ζ of nearest Lys	48	0.20	4.4
C_δ of L-Gln	N_ζ of nearest Lys	80	0.53	4.3
C_δ of L-Gln	N_ζ of nearest Lys	112	0.80	4.3

Table 3: Summary of REDOR Measured Distances and Their Counterparts from the Refined GlnBP and L-Gln Complex Structure[a]

dephasing nucleus	obsd nucleus	REDOR (Å)	refined (Å)
C_δ of L-Gln	$N_{\epsilon 2}$ of His156	4.3 ± 0.2*	4.9 ± 0.3
C_δ of L-Gln	$N_{\delta 1}$ of His156	>6.5	6.8 ± 0.3
$C_{\epsilon 1}$ of His156	N of L-Gln	6.2 ± 0.2*	5.7 ± 0.2
$C_{\epsilon 1}$ of His156	$N_{\epsilon 2}$ of L-Gln	>7*	6.6 ± 0.3
C_δ of L-Gln	N_ζ of Lys115	4.4 ± 0.2	6.9 ± 0.5
$F_{\epsilon 1}$ of Tyr143	$N_{\epsilon 2}$ of His156	8.1 ± 0.5	6.3 ± 0.4
$F_{\epsilon 2}$ of Tyr143	$N_{\epsilon 2}$ of His156		5.3 ± 0.4
$F_{\epsilon 1}$ of Tyr185	$N_{\epsilon 2}$ of His156		9.2 ± 0.5
$F_{\epsilon 2}$ of Tyr185	$N_{\epsilon 2}$ of His156		7.6 ± 0.5
$F_{\epsilon 1}$ of Tyr143	$N_{\delta 1}$ of His156	8.6 ± 0.5	6.6 ± 0.4
$F_{\epsilon 2}$ of Tyr143	$N_{\delta 1}$ of His156		4.9 ± 0.4
$F_{\epsilon 1}$ of Tyr185	$N_{\delta 1}$ of His156		9.2 ± 0.5
$F_{\epsilon 2}$ of Tyr185	$N_{\delta 1}$ of His156		7.2 ± 0.5

[a] The REDOR measured distances which were used in the molecular dynamics calculations are indicated by an asterisk.

the protein is ^{15}N-depleted. The difference spectrum represents those [^{15}N]amide nitrogens that interact with a ^{13}C neighbor via dipolar coupling. Determination of what proportion of the difference spectrum peak was due to dephasing by $^{13}C_{\epsilon 1}$ of His156 and what proportion was due to dephasing by natural-abundance, background ^{13}C nuclei was accomplished by an examination of a separate REDOR experiment performed on a control sample consisting of [U-^{14}N]GlnBP bound to L-[*amide*-^{15}N]Gln. The resulting difference spectrum was virtually identical to that from the sample with labeled histidine. Thus, the distance between $^{13}C_{\epsilon 1}$ of His156 and [^{15}N]amide of L-Gln can only be assigned a lower limit: the internuclear distance is on the order of 7 Å or greater.

^{15}N-Observed, ^{13}C-Dephased REDOR of L-[*ring*-2-^{13}C]-*His*-[*U*-^{14}N]*GlnBP* + L-[*Amine*-^{15}N]*Gln.* The results of a REDOR experiment performed on L-[*ring*-2-^{13}C]His-[U-^{14}N]-GlnBP bound to L-[*amine*-^{15}N]Gln with $N_c = 112$ rotor cycles of dephasing are shown in Figure 6a, which displays both the full-echo spectrum (bottom) and the difference spectrum (top). The full-echo spectrum is dominated by the large peak at ~10 ppm, which represents mostly [^{15}N]amine of the glutamine ligand, but may contain a small contribution from lysine $^{15}N_\zeta$ nitrogens. That other ^{15}N nitrogens are present in the protein even though the protein is ^{15}N-depleted is evidenced by the fact that a small peak representing [^{15}N]-amide nitrogens is present at the center of the spectrum. The difference spectrum in Figure 6a shows that significant dephasing of [^{15}N]amine nitrogens by ^{13}C neighbors occurs, either by $^{13}C_{\epsilon 1}$ of His156 or by background ^{13}C nuclei.

For purposes of comparison, a separate REDOR experiment performed on a control sample consisting of natural-abundance GlnBP bound to L-[*amine*-^{15}N]Gln was also performed. The results of this REDOR experiment are shown in Figure 6b, which displays the full-echo spectrum (bottom) and the difference spectrum (top). Experimental conditions are identical to those in Figure 6a. The large peak at ~10 ppm in the full-echo spectrum of Figure 6b represents mostly [^{15}N]-amine of the glutamine ligand. The substantial signal in the center of the spectrum represents normal natural-abundance [^{15}N]amide nuclei. The difference spectrum in Figure 6b reveals that the [^{15}N]amine nitrogens are dephased by background ^{13}C nuclei.

To ensure that the presence in parts a and b of Figure 6 of background ^{15}N nuclei resonating at ~10 ppm does not interfere with the analysis of the peak representing only [^{15}N]-amine of the glutamine ligand, a third REDOR experiment was performed on a sample consisting of [U-^{15}N]GlnBP bound to natural-abundance L-Gln. This experiment was performed under conditions identical to those in parts a and b of Figure

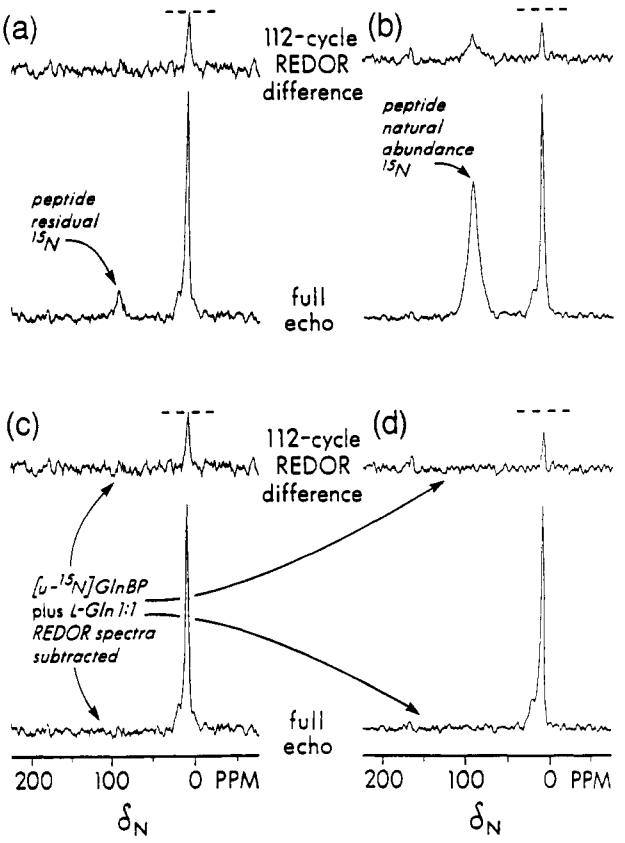

FIGURE 6: (a) ^{15}N-Observed, ^{13}C-dephased REDOR of 176 mg of L-[*ring*-2-^{13}C]His-[U-^{14}N]GlnBP bound to L-[*amine*-^{15}N]Gln with N_c = 112 rotor cycles of dephasing resulting in a full-echo spectrum (bottom) and a difference spectrum (top); both spectra used 415 296 scans. (b) ^{15}N-Observed, ^{13}C-dephased REDOR of 285 mg of natural-abundance GlnBP bound to L-[*amine*-^{15}N]Gln with N_c = 112 rotor cycles of dephasing resulting in a full-echo spectrum (bottom) and a difference spectrum (top); both spectra used 293 184 scans. (c and d) Spectra in (a and b) minus the scaled result of an identical experiment performed on [U-^{15}N]GlnBP bound to natural-abundance L-Gln. The scaling was chosen so that the difference spectra have no peptide peak at 100 ppm (arrows).

6. The full-echo spectrum and the difference spectrum that result from this third experiment were then subtracted from the corresponding spectra in parts a and b of Figure 6 to yield the spectra shown in parts c and d of Figure 6, respectively. Clearly, the peaks at ~10 ppm are virtually unchanged, but they now represent only [^{15}N]amine nitrogens of the L-Gln ligand.

Determination of what proportion of the difference spectrum peak in Figure 6c is due to dephasing by $^{13}C_{\epsilon 1}$ of His156 and what proportion is due to dephasing by natural-abundance, background ^{13}C nuclei is accomplished by examination of the difference spectrum peak in Figure 6d, which represents [^{15}N]-amine nitrogen dephased by natural-abundance, background ^{13}C nuclei.

Determination of the distance between $^{13}C_{\epsilon 1}$ of His156 and [^{15}N]amine of L-Gln by analysis of the data in parts c and d of Figure 6 is carried out as before. It is found that $\Delta S/S_c$ = 0.26 and $\Delta S/S_d$ = 0.13; $\Delta S/S_d$ is subtracted from $\Delta S/S_c$ to correct for background ^{13}C dephasing of the ^{15}N resonance; the value is multiplied by the factor M = 1.0425 derived from Figure 2 to correct for the performance of REDOR at N_c = 112 rotor cycles; $M(\Delta S/S_c - \Delta S/S_d)$ = 0.14, N_cDT_r = 0.37, D = 12 Hz, and r = 6.2 Å (Table 3). Division of $M(\Delta S/S_c - \Delta S/S_d)$ by L is not necessary because the nucleus observed is part of the ligand in this case.

Table 4: Summary of REDOR Distances Measured with the L-[*m*-^{19}F]Tyr-[U-^{15}N]GlnBP + L-[5-^{13}C]Gln Sample[a]

dephasing nucleus	obsd nucleus	rotor cycles of dephasing	$\Delta S/S_0$	REDOR distance (Å)
C_δ of L-Gln	$N_{\epsilon 2}$ of His156	80	0.46	4.6 ± 0.2
$F_{\epsilon 1}$ or $F_{\epsilon 2}$ of Tyr	$N_{\epsilon 2}$ of His156	120	0.39	8.1 ● 0.5
$F_{\epsilon 1}$ or $F_{\epsilon 2}$ of Tyr	$N_{\delta 1}$ of His156	120	0.28	8.6 ± 0.5

[a] All calculations involving ^{19}F nuclei were done under the assumption that only one ^{19}F nucleus was involved in the dephasing of the REDOR signal.

^{15}N-Observed, ^{13}C-Dephased REDOR of [ring-3-^{19}F]Tyr-[U-^{15}N]GlnBP + L-[*5-^{13}C*]*Gln*. A REDOR experiment was first performed to provide evidence that fluorination does not affect the structure near His156 and the L-Gln ligand. Therefore, ^{15}N-observed, ^{13}C-dephased REDOR was performed on [*m*-^{19}F]Tyr-[U-^{15}N]GlnBP bound to L-[5-^{13}C]Gln with N_c = 80 rotor cycles of dephasing. The results are summarized in Table 4 and are in agreement with REDOR results on the nonfluorinated sample of Figures 4 and 5. In fact, if the results shown in Figure 5 (right) are also used to indicate the magnitude of background dephasing of ^{15}N by ^{13}C for the fluorinated sample, then analysis to determine the distance between $^{15}N_{\epsilon 2}$ of His156 and $^{13}C_\delta$ of L-Gln shows that $\Delta S/S$ = 0.46, $\Delta S/S_{5b}$ = 0.17, and $(\Delta S/S - \Delta S/S_{5b})/L$ = 0.35 and that N_cDT_r = 0.62, D = 29 Hz, and r = 4.6 Å. The fluorinated sample appears to yield a $^{15}N_{\epsilon 2}$ of His156 to $^{13}C_\delta$ of Gln distance that is 0.2–0.3 Å longer than that found in the nonfluorinated sample. The L = 0.814 is determined by comparisons of ^{13}C-CPMAS-echo spin counts of the carbonyl carbons of this particular sample and the sample used in Figure 5 (right).

^{15}N-Observed, ^{19}F-Dephased REDOR of [ring-3-^{19}F]Tyr-[U-^{15}N]GlnBP + L-[*5-^{13}C*]*Gln*. The results of the ^{15}N-observed, ^{19}F-dephased REDOR experiment performed on [*m*-^{19}F]Tyr-[U-^{15}N]GlnBP bound to L-[$^{13}C_\delta$]Gln with N_c = 120 rotor cycles of dephasing are also presented in Table 4. Analysis of the data to determine the distance between $^{15}N_{\delta 1}$ of His156 and $^{19}F_{\epsilon 1}$ or $^{19}F_{\epsilon 2}$ of Tyr and the distance between $^{15}N_{\epsilon 2}$ of His156 and $^{19}F_{\epsilon 1}$ or $^{19}F_{\epsilon 2}$ of Tyr is predicated on the assumption that only one Tyr residue is involved in the interaction with $^{13}C_\delta$ of Gln and that the ring of this Tyr does not flip. For the distance between $^{15}N_{\delta 1}$ of His156 and $^{19}F_{\epsilon 1}$ or $^{19}F_{\epsilon 2}$ of Tyr, data analysis indicates $\Delta S/S$ = 0.28 for the peak area at ~220 ppm, N_cDT_r = 0.54, D = 17 Hz, and the internuclear average distance r = 8.6 Å according to the formula $r = (10825/D)^{1/3}$. For the distance between $^{15}N\epsilon_2$ of His156 and $^{19}F_{\epsilon 1}$ or $^{19}F_{\epsilon 2}$ of Tyr, data analysis indicates $\Delta S/S$ = 0.39 for the peak area at ~140 ppm, NDT_r = 0.66, D = 21 Hz, and the internuclear distance r = 8.1 Å according to the formula $r = (10825/D)^{1/3}$. Since both Tyr and His are present as part of the protein molecule, the percentage of isotopically labeled substrate present in the protein–ligand complex is not a factor. Also, since ^{19}F is not otherwise found in the protein, dephasing of ^{15}N nuclei by background ^{19}F nuclei is nonexistent.

Molecular Refinement

The energy-minimization procedures used involved 200 steps of the steepest decents method and an additional 250 steps of the conjugate gradient method (Flectcher & Reeves, 1964). The potential energy of the complex system converges rapidly. It reached close to a minimum after the first 200 time steps of the steepest descents algorithm, suggesting the subsequent

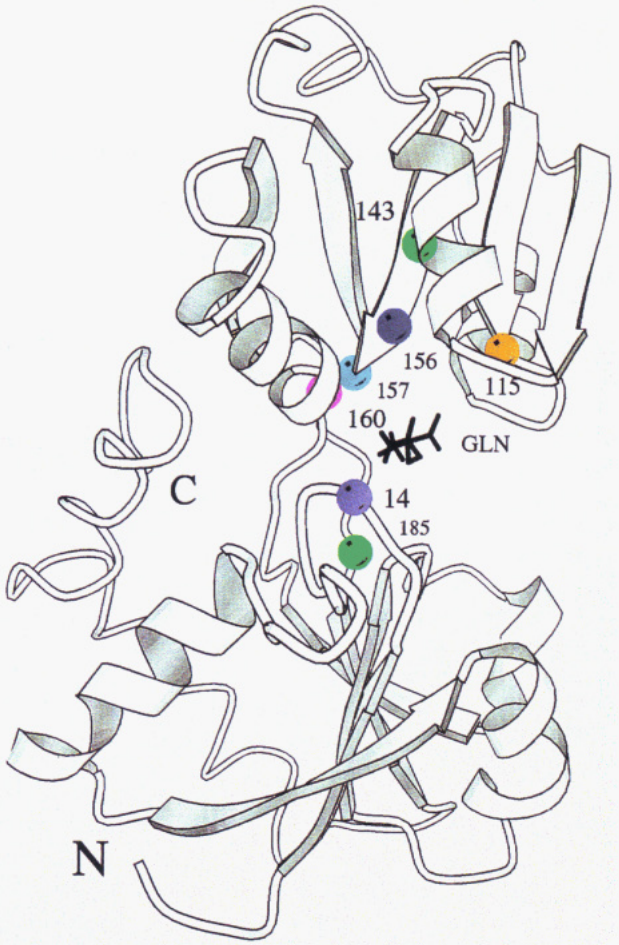

FIGURE 7: Relative positions of the His156 residue and L-Gln ligand with respect to the whole protein. This is the structure prior to energy minimization, represented by the ribbon picture of the polypeptide backbone using Molscript (Kraulis, 1991).

250 time steps of the conjugate-gradient part of the energy minimization to be unnecessary.

The relative orientation of the His156 and the L-Gln ligand with respect to the whole protein molecule is illustrated in Figure 7. The bilobal structure of the GlnBP is also illustrated in Figure 7, which contains the "small" and "large" domains (Hsiao, 1993; Hsiao *et al.*, 1994). The His156 residue is within the small domain of the GlnBP. The L-Gln ligand sits closer to the interior, thus closer to the hinge of the binding cavity. Comparison of the overall distance across the cavity was made between the initial structure (without the ligand) and the refined structure (with the ligand). This was done by measuring the distance between the C_α of Val14 in the large domain and Ile139 in the small domain. The initial distance was 14.96 Å compared to the refined distance of 10.74 Å (Figure 8a). The difference of 4.22 Å seems rather small compared to the hinge-bending process observed with other binding proteins. In addition, the total solvent-accessible surface of L-Gln was reduced only by 2% after refinement. Figure 8b shows the local binding-site geometry as well as the possible network of inter- and intramolecular hydrogen bonds. The orientation of the L-Gln ligand is almost perpendicular to the imidazole plane of His156. Two intermolecular hydrogen-bond formations between the $N_{\epsilon 2}$-H of His156 as well as N_ζ-H of Lys115 and the α-carboxyl oxygens of L-Gln can be observed. Similarly, intermolecular hydrogen bonds to the L-Gln ligand are formed from Asp157 and Asn160 in the small domain as well as from Tyr185 and Val14 in the large domain. The distance between C_δ of L-Gln and the N_ζ of Lys115, which is the nearest lysine residue, is 6.9 Å, as determined from the refined structure. The values obtained for side-chain torsion angles for L-Gln, $\chi_1 = -172.4°$ and $\chi_2 = 67.6°$, seem to agree with values in the rotamer library of Ponder and Richards (1987) for L-Gln ($\chi_1 = -179.4°$ and $\chi_2 = 67.3°$ with standard deviations of 21.5° and 7.9° for χ_1 and χ_2, respectively).

A summary of the distances obtained from the refined calculated structure of the complex and the comparison with their counterparts from REDOR experiments are given in Table 3. These distances are determined from the average structure over the 20-ps molecular dynamics calculation. The deviations from the average structure are the root-mean-square fluctuation amplitudes. These distances are in reasonable agreement with the values obtained by REDOR NMR. Local geometry around the His156 and L-Gln ligand is naturally determined with a higher certainty than that farther away from the source of the REDOR-determined constraints.

DISCUSSION

Histidine-156. The refined structure of the GlnBP and L-Gln complex shows that the $N_{\epsilon 2}$-H of His156 forms an intermolecular hydrogen bond with the α-carboxyl of L-Gln (Figure 8b). This is a direct confirmation of the earlier proposal that the $N_{\epsilon 2}$-H of His156 is involved in formation of a hydrogen bond with L-Gln (Tjandra *et al.*, 1992). However, the refined structure suggests that α-carboxyl is the hydrogen acceptor instead of γ-carbonyl, as previously predicted. The earlier model was derived from proton exchange as well as NOE studies (Shen, 1988). Even though the earlier model could fit the exchange and NOE data, the results of glutamine analog studies by Shen *et al.* (1989a) could not be explained. In those experiments, all of the analogs which bind to GlnBP had alterations on the γ-carbonyl end instead of the α-carboxyl side, suggesting that the latter is more important to binding specificity. The model of Figure 8b explains both the exchange and NOE data as well as the analog results. Furthermore, the hydrogen-bond networks around both the α-carboxyl and the amide ends of L-Gln illustrate possible additional constraints for the selectivity of ligand binding to the protein. This model also suggests how the overall geometry around the binding site may play an important role in ligand specificity.

A 0.2–0.3-Å longer distance observed between the $N_{\epsilon 2}$ of His156 and C_δ of L-Gln in the $^{19}F_{\epsilon 1}$ of Tyr and ^{15}N-uniformly labeled GlnBP sample is not unexpected. Earlier investigations of ^{19}F labeling of proteins (Rule *et al.*, 1987; Peersen *et al.*, 1990) have suggested slight conformational changes from the native form. This is due primarily to the fact that the van der Waals radius of ^{19}F nuclei is about 30% larger than ^1H nuclei. However, no noticeable changes in activities or physical properties of the systems were observed. In the case of GlnBP, a high-resolution ^1H-NMR spectrum of the sample was taken as a control during the last stage of the sample preparation, which showed the ability of the ^{19}F-labeled protein to bind ligand. Thus, this slight conformational change does not seem to alter the ligand-binding properties of GlnBP. The distances of 8.1 ± 0.1 and 8.6 ± 0.1 Å from the $N_{\epsilon 2}$ and $N_{\delta 1}$ of His156, respectively, to the nearest $F_{\epsilon 1}$ of Tyr were calculated under the assumption that there is only one tyrosine involved in the dephasing of the ^{15}N resonances. From the refined model, one can conclude that these distances could be associated with either of two tyrosine residues: Tyr143 or Tyr185. Further investigations of individual contributions to the total observed amount of the ^{15}N-signal dephasing must be done in order to be able to use these tyrosines as constraints in the molecular

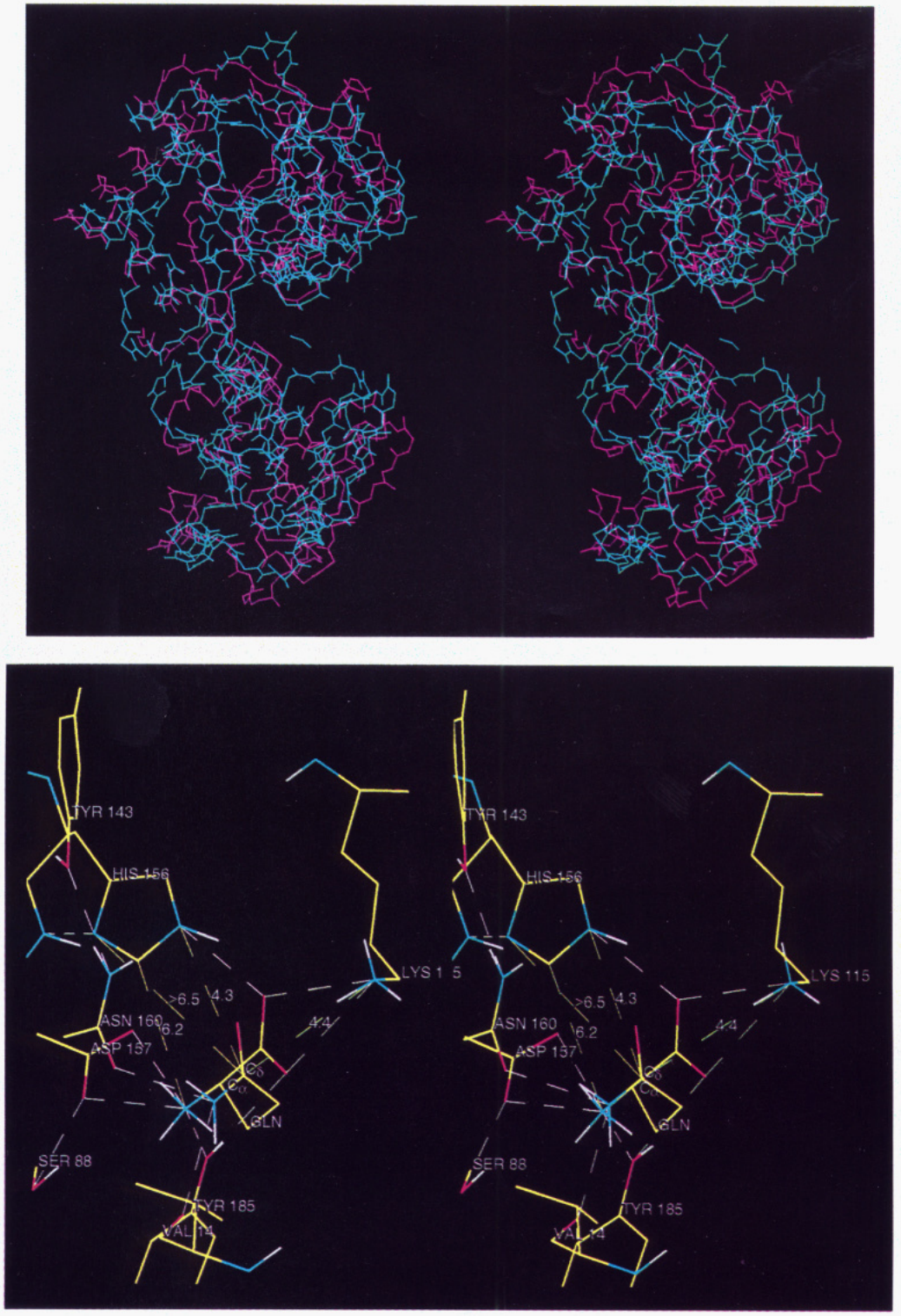

FIGURE 8: (a, top) Stick diagram of the polypeptide chain of the GlnBP–Gln structure before (magenta) and after (cyan) a 20-ps molecular dynamics calculation with energy minimization. (b, bottom) Stick diagram illustrating the binding-site conformation of the refined GlnBP–Gln structure within a 10-Å radius of C_δ of L-Gln. The white dashed lines represent possible hydrogen bonds, while the green dashed lines indicate REDOR-measured distances. Both figures were obtained by the XFIT program (McRee, 1992).

dynamics calculation. At this stage, however, the results from the molecular dynamics calculation and the REDOR experiments can be used as clear indications that there is at least one tyrosine residue in proximity to the binding site.

Lysine-115. Both the REDOR and molecular refinement methods clearly suggest that there is one lysine residue in proximity to the binding site; the simulations indicate that it is most likely Lys115. The constraints used do not permit one to conclude with certainty how Lys115 is oriented with respect to L-Gln. Qualitatively, however, the results of the molecular dynamics calculation favor the placement of N_ζ of Lys115 within 6.9 Å of the C_δ of L-Gln. This is solely on the basis of an acceptable total energy. Meanwhile, the REDOR experiment has independently provided a distance of about 4.3 Å. Note that this measured distance was not included as a constraint in the molecular dynamics calculation since there was no definite proof as to which lysine is dephased by the $^{13}C_\delta$-L-Gln. The calculation was done under the assumption

that no gross structural changes occur within each individual domain. Known crystal structures of periplasmic proteins show that indeed neither domain experiences large structural changes. However, the orientation of one domain relative to the other changes significantly as the protein closes upon ligand binding (Oh *et al.*, 1993). For residues located within the small domain, we believe that the calculated distances are reliable because they do not depend on the open or closed form of the protein. In contrast, interdomain distances do depend on the open or closed form of the protein, and since no unambiguous REDOR-measured, interdomain distances are available at this time, care must be taken in interpreting the calculated distances. Carefully designed mutant proteins of GlnBP will provide new REDOR probes to allow interdomain distances to be measured. These interdomain distances, combined with simulations using molecular refinement, should lead to a better structure of the protein–ligand complex than is now available.

Large and Small Domains. Recent published results on crystal structures of periplasmic proteins suggest several possible models for ligand binding in GlnBP (Hsiao, 1993; Hsiao *et al.*, 1994; Oh *et al.*, 1993). Oh *et al.* (1993) determined a possible ligand-binding conformation in GlnBP using lysine–arginine–ornithine-binding protein as the starting structure. A conformation was suggested where Lys115 in the small domain defines the specificity of GlnBP for L-Gln *via* its amido group. Furthermore, the residues Asp73 in the large domain and Asp157 in the small domain of GlnBP act as charge neutralizers and stabilizers at the carboxyl and amino groups of the ligand, respectively (Oh *et al.*, 1993). Our model is in excellent agreement with that of Oh *et al.* (1993) regarding the possible function of Lys115. In addition, Asp157 is involved in ligand binding in both models. There are two possible hypotheses for Asp157: (i) it is a charge stabilizer for the amino group of the L-Gln, in agreement with Oh *et al.* (1993); or (ii) it is a His156 ring stabilizer through an intramolecular hydrogen-bond interaction (Figure 8b). Both the REDOR-NMR as well as earlier ^{1}H-NMR (Shen *et al.*, 1989a) experiments have suggested the involvement of His156 in ligand binding in GlnBP. By comparison, Hsiao (1993) and Hsiao *et al.* (1994) arrived at two possible models for the liganded form of GlnBP. In the first model, they proposed Phe50 in the large domain and Lys115 in the small domain as hydrogen donors and Asp10 in the large domain as a hydrogen acceptor, in addition to His156, in hydrogen-bond network formation. In the second model, they proposed Asp10 and Phe50 in the large domain as well as Thr118 and His156 in the small domain to be involved in ligand binding. Further investigation is obviously needed to clarify whether, in fact, Asp10, Phe50, Asp73, and Thr118 are involved in ligand binding.

Hinge Region. Earlier biochemical (Hunt & Hong, 1983b) as well as spectroscopic studies (Shen *et al.*, 1989b) of the tryptophan residues in GlnBP have suggested their involvement in translocation of the L-Gln ligand across the membrane. Specifically, the presence of Trp220, which is located near the carboxy terminus and close to the hinge of the GlnBP structure, affects the ability of the GlnBP–Gln complex to complete the transport process efficiently (Hunt & Hong, 1983b; Shen *et al.*, 1989b). Our model suggests that the L-Gln ligand is located deep inside the binding pocket but is not yet fully sequestered. In order for the protein to undergo a more complete hinge-bending motion to arrive at the final closed form of the complex, some amino acid residues near the hinge should experience conformational changes (Newcomer *et al.*, 1981; Mao *et al.*, 1982). Perhaps establishing stable-isotope probes between the ligand and Trp220 at the hinge of the protein would facilitate specifiying the structural features needed for recognition of the GlnBP–Gln complex by the membrane-associated components of the glutamine transport system (Ames, 1986; Quiocho, 1990). Interdomain distances close to the binding pocket opening as well as to the hinge are needed to specify the hinge bending. The combination of these distances might then provide a more plausible closed structure of the GlnBP–Gln complex than that of Figure 8.

Conclusion. The data in this paper illustrate the application of REDOR NMR in determining internuclear distances in a solid form of a protein–ligand complex. This method is not limited by the size or the dynamic properties of the protein molecule. Different combinations of specific isotope labeling can be chosen to minimize background interferences and to provide an efficient way of obtaining detailed structural information. Combining this method of distance measurement with molecular dynamics calculations provides a new analytical method for selecting an acceptable protein structure.

ACKNOWLEDGMENT

We thank Dr. Chwan-Deng Hsiao, Ms. Yuh-Ju Sun, Dr. John Rose, and Dr. Bi-Cheng Wang for providing the crystal structure of GlnBP prior to publication and for several helpful discussions of the structure of the unliganded form of GlnBP. We also thank the National Stable Isotope Resources at the Los Alamos National Laboratory for providing a sample of the L-[*ring*-2-^{13}C]histidine. The double-labeled emirimicin fragment used in the calibration experiment of Figure 2 was generously provided by Dr. G. R. Marshall (Washington University School of Medicine). The fragment was designed by Dr. D. D. Beusen (Washington University School of Medicine) and synthesized by Drs. K. Kociolek and A. S. Redlinski under the direction of Dr. M. T. Leplawy (Polish Academy of Sciences). Finally, we thank Dr. E. Ann Pratt for her valuable comments on the manuscript.

REFERENCES

Ames, G. F.-L. (1986) *Annu. Rev. Biochem. 55*, 397–425.
Ames, G. F.-L., Mimura, C. S., & Shyamala, V. (1990) *FEMS Microbial. Rev. 75*, 429–446.
Bax, A., & Grzesiek, S. (1993) *Acc. Chem. Res. 26*, 131–138.
Boelens, R., Koning, T. M. G., & Kaptein, R. (1988) *J. Mol. Struct. 173*, 299–311.
Boelens, R., Koning, T. M. G., van der Marel, G. A., van Boom, J. H., & Kaptein, R. (1989) *J. Magn. Reson. 82*, 290–308.
Chen, P., Rose, J., Chung, Y. J., Wang, B., Shen, Q., Cottam, P. F., & Ho, C. (1989) *J. Mol. Biol. 205*, 459–460.
Christensen, A. M., & Schaefer, J. (1993) *Biochemistry 32*, 2868–2873.
Clore, G. M., & Gronenborn, A. M. (1991) *Science 252*, 1390–1399.
Flectcher, R., & Reeves, C. M. (1964) *Comput. J. 7*, 149.
Gullion, T., & Schaefer, J. (1989) *J. Magn. Reson. 81*, 196–200; *Adv. Magn. Reson. 13*, 57–83.
Gullion, T., Baker, D. B., & Conradi, M. S. (1990) *J. Magn. Reson. 89*, 479–484.
Holl, S. M., Marshall, G. R., Beusen, D. D., Kociolek, K., Redlinski, A. S., Leplawy, M. T., McKay, R. A., Vega, S., & Schaefer, J. (1992) *J. Am. Chem. Soc. 114*, 4830–4833.
Hsiao, C.-D. (1993) Crystallographic Analysis of Glutamine-Binding Protein, Ph.D. Thesis, University of Pittsburgh, Pittsburgh, PA.
Hsiao, C.-D., Sun, Y.-J., Rose, J., Cottam, P. F., Ho, C., & Wang, B.-C. (1994) *J. Mol. Biol.* (in press).

Hunt, A. G., & Hong, J.-S. (1981) *J. Biol. Chem. 256*, 11988–11991.
Hunt, A. G., & Hong, J.-S. (1983a) *Biochemistry 22*, 844–850.
Hunt, A. G., & Hong, J.-S. (1983b) *Biochemistry 22*, 851–854.
Hyde, S. G., Emsley, P., Hartshorn, M. J., Mimmack, M. M., Gileadi, U., Pearce, S. R., Gallagher, M. P., Gill, D. R., Hubbard, R. E., & Higgins, C. F. (1990) *Nature 346*, 362–365.
Koning, T. M. G. (1990) IRMA: Iterative relaxation matrix approach for NMR structure determination. Application to DNA fragments, Ph.D. Thesis, University of Utrecht, The Netherlands.
Kraulis, P. (1991) *J. Appl. Crystallogr. 24*, 946–950.
Kreishman, G. P., Robertson, D. E., & Ho, C. (1973) *Biochem. Biophys. Res. Commun. 53*, 18–23.
Luecke, H., & Quiocho, F. A. (1990) *Nature 347*, 402–406.
Mao, B., Pear, M. R., McCammon, J. A., & Quiocho, F. A. (1982) *J. Biol. Chem. 257*, 1131–1133.
Marshall, G. R., Beusen, D. D., Kociolek, K., Redlinski, A. S., Leplawy, M. T., Pan, Y., & Schaefer, J. (1990) *J. Am. Chem. Soc. 112*, 963–966.
McDowell, L. M., Holl, S. M., Qian, S.-J., Li, E., & Schaefer, J. (1993) *Biochemistry 32*, 4560–4563.
McRee, D. E. (1992) *J. Mol. Graphics 10*, 44–46.
Neu, H. C., & Heppel, L. A. (1965) *J. Biol. Chem. 240*, 3685–3692.
Newcomer, M. E., Lewis, B. A., & Quiocho, F. A. (1981) *J. Biol. Chem. 256*, 13218–13222.
Nohno, T., Saito, T., & Hong, J. (1986) *Mol. Gen. Genet. 205*, 260–269.
Oh, B.-H., Kang, C.-H., De Bondt, H., Kim, S.-H., Nikaido, K., Joshi, A. K., & Ames, G. F.-L. (1993) *J. Biol. Chem. 268*, 11348–11355.
Pan, Y., Gullion, T., & Schaefer, J. (1990) *J. Magn. Reson. 90*, 330–340.
Peersen, O., Pratt, E. A., Truong, H.-T. N, Ho, C., & Rule, G. S. (1990) *Biochemistry 29*, 3256–3262.
Ponder, J. W., & Richards, F. M. (1987) *J. Mol. Biol. 193*, 775–791.
Quiocho, F. A. (1990) *Philos. Trans. R. Soc. London, B 326*, 341–351.
Rance, M., & Byrd, R. A. (1983) *J. Magn. Reson. 52*, 221–240.
Rule, G. S., Pratt, E. A., Simplaceanu, V., & Ho, C. (1987) *Biochemistry 26*, 549–556.
Schmidt, A., Cohen, E. C., McDowell, L. M., Beusen, D. D., & Schaefer, J. (1993) 34th Experimental NMR Conference, St. Louis, MO.
Shen, Q. (1988) Biochemical, Biophysical, and Molecular Genetic Studies on Glutamine Binding Protein from *Escherichia coli*, Ph.D. Thesis, Carnegie Mellon University, Pittsburgh, PA.
Shen, Q., Simplaceanu, V., Cottam, P. F., & Ho, C. (1989a) *J. Mol. Biol. 210*, 849–857.
Shen, Q., Simplaceanu, V., Cottam, P. F., Wu, J., Hong, J., & Ho, C. (1989b) *J. Mol. Biol. 210*, 859–867.
Shore, S. E., Ansermet, J. P., & Slichter, C. P. (1987) *Phys. Rev. Lett. 58*, 953–956.
Tjandra, N. (1993) Structural studies of glutamine binding protein of *Escherichia coli* using multidimensional magnetic resonance Ph.D. Thesis, Carnegie Mellon University, Pittsburgh, PA.
Tjandra, N., Simplaceanu, V., Cottam, P. F., & Ho, C. (1992) *J. Biomol. NMR 2*, 149–160.
van Gunsteren, W. F., & Berendsen, H. J. C. (1977) *Mol. Phys. 34*, 1311–1327.
Verlet, L. (1967) *Phys. Rev. 159*, 98–103.
Vyas, N. K., Vyas, M. N., & Quiocho, F. A. (1983) *Proc. Natl. Acad. Sci. U.S.A. 80*, 1792–1796.
Weiner, J. H., & Heppel, L. A. (1971) *J. Biol. Chem. 246*, 6933–6941.
Willis, R. C., Iwata, K. K., & Furlong, C. E. (1975) *J. Bacteriol. 122*, 1032–1037.
Wüthrich, K. (1986) *NMR of Proteins and Nucleic Acids*, John Wiley and Sons, Inc., New York.
Wüthrich, K. (1989) *Science 243*, 45–50.